Journal of Molecular Graphics and Modelling 72 (2017) 1–5

Contents lists available at ScienceDirect

Journal of Molecular Graphics and Modelling

journal homepage: www.elsevier.com/locate/JMGM

Optimized Tersoff empirical potential for germanene

Sayyed Jalil Mahdizadeh*, Golnoosh Akhlamadi

Department of Chemistry, Ferdowsi University of Mashhad, Mashhad 91779, Iran

ARTICLE INFO

Article history:
Received 17 October 2016
Received in revised form
14 November 2016
Accepted 16 November 2016
Available online 13 December 2016

Keywords:
Optimized Tersoff potential
Germanene
Molecular dynamics simulation

ABSTRACT

In the current work, the issue of re-parameterization of Tersoff empirical potential model was addressed for 2D nanomaterial 'germanene' to be applied in molecular dynamics simulation based studies. The well-known chi-square minimization procedure was used to optimize the original Tersoff potential parameters. Many properties of germanene were extracted using both original and optimized Tersoff potentials and they compared with the corresponding density functional theory data. According to the results, the optimized Tersoff potential provides a significant improvement in many structural, thermodynamic, mechanical, and thermal properties of geramanene.

© 2016 Elsevier Inc. All rights reserved.

1. Introduction

Two-dimensional (2D) materials are one of the most active areas of nanomaterials research due to their fascinating mechanical, electronic, and transport properties [1–3]. 2D nanomaterials have a potential application for integration into the next-generation electronic and energy conversion devices [4,5]. Graphene, the most widely studied 2D material, possesses extreme mechanical strength, [6] exceptionally high electrical [7] and thermal conductivities [8], as well as many other supreme properties [3]. Recently, the other 2D group-IV nanomaterial, germanene, has been realized by epitaxial growth on substrates [9–11] and attracted rigorous interest due to its exceptional properties.

Germanene, graphene's cousin, is a single layer of germanium forming a 2D honeycomb lattice. Although germanium and carbon are in the same group IV of the periodic table, there are a large differences in their chemical and structural properties regarding to their orbital hybridization state. Carbon makes sp and sp^2 hybridization easily, while germanium atoms prefer to bond each other with mainly sp^3 hybridization [12]. There are two well-known reasons for this difference in hybridization. Firstly, the energy required for hybridization of s and p orbitals in germanium is much smaller than that in carbon. Therefore, it makes much less energy needs in germanium to hybridize all of its three p orbitals with s orbitals to make sp3 configuration [12]. In addition, Ge–Ge bond length (2.44 Å) [13] is much larger than the C—C bond length (1.42 Å) [8] thus making the p_z overlapping and hence the π bond formation more difficult in germanium.

The mixed sp^2 and sp^3 hybridization in germanene results in a prominent buckling structure (0.74 Å) [14], in contrast to perfect planar graphene, which opens an electrically tunable band gap [15]. Also, the transport and mechanical properties of germanene are strongly affected by this buckling feature. As a consequence, it is a huge advantage as compared to graphene, i.e. in thermoelectric nano-devices and flexible nano-electronics [16].

Until now, the computational methods employed to study the germanene properties are restricted to ab initio and density functional theory (DFT) calculations [17–21]. However, the use of quantum atomistic approaches is precluded by the size of the nanostructure which is normally several orders of magnitude larger than that of the largest simulation cell of a typical ab initio/DFT calculations. On the other hand, the development of atomistic empirical potential (EP) methods for molecular dynamics (MD) simulation has long allowed large scale structural simulations of low dimensional IV semiconductor materials [22]. Because of computational time and cost, the typical number of atoms that is possible to simulate with MD simulation based on the empirical methods greatly exceeds that of ab initio/DFT methods, albeit at the cost of accuracy.

The most commonly used EPs are those developed by Tersoff for groups III, IV and V elements [23–26]. The convenience of the Tersoff EP comes from its rather simple, analytical form and the short range of atomic interactions. During the investigation of germanene using MD simulation based of the Tersoff EP, it revealed that original Tersoff EP for germanium could not accurately reproduce the DFT data regarding structural, mechanical, and transport properties of germanene as a new 2D nanostructure of germanium.

* Corresponding author.
E-mail address: saja.mahdizadeh@gmail.com (S.J. Mahdizadeh).

http://dx.doi.org/10.1016/j.jmgm.2016.11.009
1093-3263/© 2016 Elsevier Inc. All rights reserved.

Table 1
Original Tersoff EP parameters for germanium [23].

$A = 1769.0$ eV	$B = 419.23$ eV	$\lambda_1 = 2.4451$ Å^{-1}
$\lambda_2 = 1.7047$ Å^{-1}	$\lambda_3 = 0.000$ Å^{-1}	$n = 0.75627$
$C = 106430$	$\beta = 9.0166\times10^{-7}$	$d = 15.652$
$\cos\theta_0 = -0.43884$	$R = 2.8$ Å	$D = 0.3$ Å
$m = 3$	$\gamma_{ijk} = 1$	

Here, we are going to achieve to an effective set of parameters to reproduce most structural, thermodynamics, mechanical, and thermal properties of geramanene with a good agreement compared with DFT results. The current study was inspired from the similar work by Lindsay and Broido [27], where they successfully introduced an alternate set of Tersoff potential parameters for better description of lattice dynamics and phonon thermal transport in carbon nanotubes and graphene.

2. Tersoff EP model

The analytical form for the pair potential, V_{ij}, of the Tersoff EP model [24] is given by the following functions with the corresponding original parameters listed in Table 1 [23].

$$V_{ij} = f_C(r_{ij})\left[a_{ij}f_R(r_{ij}) + b_{ij}f_A(r_{ij})\right] \tag{1}$$

$$f_R(r_{ij}) = A\ \exp(-\lambda_1 r_{ij}) \tag{2}$$

$$f_A(r_{ij}) = -B\ \exp(-\lambda_2 r_{ij}) \tag{3}$$

where r_{ij} is the distance between atoms i and j, f_R is repulsive pairwise term, which includes the orthogonalization energy when atomic wave functions overlap, and f_A is attractive pairwise terms associated with bonding. f_C is a smooth cutoff function, to limit the range of the potential to only nearest-neighbor interactions [27]. The cutoff function is defined as:

$$f_C(r_{ij}) = \begin{cases} 1 & r_{ij} < \mathrm{R} - \mathrm{D} \\ \frac{1}{2} - \frac{1}{2}\sin\left[\frac{\pi}{2}\frac{r_{ij}-R}{D}\right] & \mathrm{R}-\mathrm{D} < r_{ij} < \mathrm{R}+\mathrm{D} \\ 0 & r_{ij} > \mathrm{R}+\mathrm{D} \end{cases} \tag{4}$$

which has continuous value and derivative for all r, and goes from 1 to 0 in a small range around R. R is chosen to include only the first-neighbor shell for most structures of interest. a_{ij} (Eq. (1)), is a range-limiting term on the repulsive potential that is typically set equal to 1 [27]. The bond angle term, b_{ij}, represents a measure of the bond order, and it depends on the local coordination of atoms around atom i and the angle between atoms i, j, and k [27],

$$b_{ij} = \left(1 + \beta^n \zeta_{ij}^n\right)^{-\frac{1}{2n}} \tag{5}$$

$$\zeta_{ij} = \sum_{k\neq i,j} f_C(r_{ik})g(\theta_{ijk})\exp\left[\lambda_3^m\left(r_{ij} - r_{ik}\right)^m\right] \tag{6}$$

$$g(\theta_{ijk}) = \gamma_{ijk}\left[1 + \frac{c^2}{d^2} - \frac{c^2}{d^2 + \left(\cos\theta_{ijk} - \cos\theta_0\right)}\right] \tag{7}$$

where θ_{ijk} is the angle between atoms i, j, and k. The bond angle term lets the Tersoff EP to model the strong covalent bonding that occurs in group IV elements like carbon, silicon, and germanium systems. This angle-dependent term also allows for description of systems that bond in different geometries, such as tetrahedrally bonded diamond structure like bulk germanium or the tri-bonded germanene [27,28].

3. Fitting procedure

The well-known chi-square minimization procedure [29] was used to optimize the original Tersoff EP parameters for germanene. The chi-square (χ^2) is given by:

$$\chi^2 = \sum_i \left[\frac{\xi_i - \xi}{\xi}\right]^2 \tag{8}$$

where ξ s are high level DFT parameters used for fitting process and ξ_i are the corresponding values obtained from Tersoff EP. Here, we are going to achieve to an effective set of parameters to reproduce most structural, thermodynamics, mechanical, and thermal properties of geramanene with a good agreement compared with DFT results. Parameters used in the fitting procedure are: lattice constant, bond length and bond angle, buckling height, cohesive energy, phonon frequencies (ω_λ) and velocities ($\nu_\lambda = \partial\omega_\lambda/\partial\vec{q}$) of germanene in the high-symmetry directions. Here, $\lambda = (\vec{q}, b)$ designates a phonon with wave vector, $\vec{q}$, in branch, b.

4. Computational methods

All MD simulations were performed using LAMMPS (Large-scale Atomic/Molecular Massively Parallel Simulator) molecular dynamics code [30]. The velocity Verlet algorithm was applied to integrate the equations of motion with a fixed time step of 1 fs. The periodic boundary conditions (PBC) were applied in X and Y (in-plane) directions. All simulations were initially run for 1 ns in *NPT* ensemble (Nose–Hoover thermostat and barostat) at zero pressure and desired temperature to fully relax the initial structure and to release any undesired structural tensions.

The mechanical and elastic properties of germanene were calculated using the strain energy method [31]. We focused on the harmonic range of the elastic deformation, where the structure responded to strain (ε) linearly i.e. $-1\% \leq \varepsilon \leq 1\%$. For this, a small engineering strain was applied in both X (ε_x) and Y (ε_y) directions with constant strain rate of 0.01 ps^{-1} and the corresponding strain energy (E_s) was calculated at each point. Strain energy is defined by the following equation [31]:

$$E_s(\varepsilon_x, \varepsilon_y) = E_T(\varepsilon_x, \varepsilon_y) - E_T^0(\varepsilon_x = \varepsilon_y = 0) \tag{9}$$

where E_T and E_T^0 are total energy of strained and relaxed (unstrained) structures, respectively. The generated mesh of data corresponding to the strains in X and Y directions versus strain energy was fitted to a two-dimensional quadratic polynomial expressed by

$$E_s(\varepsilon_x, \varepsilon_y) = a_1\varepsilon_x^2 + a_2\varepsilon_y^2 + a_3\varepsilon_x\varepsilon_y \tag{10}$$

Due to the isotropy of the honeycomb structure $a_1 \simeq a_2$. The elastic tensors could be calculated in terms of fitting parameters of Eq. (9), namely, $C_{11} = \frac{2}{S_0}a_1$ and $C_{12} = \frac{1}{S_0}a_3$. S_0 is the equilibrium area. The in-plane stiffness (C), Young modulus (Y), and Poisson's ratio (ν) are related to the elastic tensors by the following equations [31],

$$C = \frac{C_{11}^2 - C_{12}^2}{C_{11}} \tag{11}$$

$$Y = \frac{1}{h}\frac{C_{11}^2 - C_{12}^2}{C_{11}} = \frac{1}{h}C \tag{12}$$

$$\nu = \frac{C_{12}}{C_{11}} \tag{13}$$

where h is the effective thickness of germanene which is determined as equilibrium van der Waals interaction distance (4.22 Å) [21].

Table 2
Optimized Tersoff EP parameters for germanene.

$A = 1760.1$ eV	$B = 430.0$ eV	$\lambda_1 = 2.4451$ Å^{-1}
$\lambda_2 = 1.71$ Å^{-1}	$\lambda_3 = 0.000$ Å^{-1}	$n = 0.75627$
$C = 106430$	$\beta = 5.017 \times 10^{-7}$	$d = 15.2$
$\cos\theta_0 = -0.35$	$R = 2.95$ Å	$D = 0.15$ Å
$m = 3$	$\gamma_{ijk} = 1$	

The phonon frequencies are determined by diagonalization of the dynamical matrix for a given $\vec{q}$ in the two-dimensional germanene Brillouin zone. The dynamical matrix was calculated from molecular dynamics simulations based on the fluctuation-dissipation theory [32] for $10 \times 10 \times 1$ super-cell with total simulation time of 5 ns. Based on the fluctuation-dissipation theory, the force constant coefficients of the system in reciprocal space are given by [32]:

$$\Phi_{\kappa\alpha,\kappa'\beta}(\vec{q}) = k_B T G^{-1}_{\kappa\alpha,\kappa'\beta} \tag{14}$$

where k_B, T, and G are Boltzmann constant, temperature, and the Green's functions, respectively. κ stands for k_{th} atom in the unit cell in reciprocal space at $\vec{q}$. $\acute{\alpha}$ and β are Cartesian components. The Green's functions coefficients can also be measured according to the following formula,

$$G_{\kappa\alpha,\kappa'\beta}(\vec{q}) = \langle R_{\kappa\alpha}(\vec{q}).R^*_{k'\beta}(\vec{q})\rangle - \langle R\rangle_{\kappa\alpha}(\vec{q}).\langle R\rangle^*_{\kappa'\beta}(\vec{q}) \tag{15}$$

where R is the instantaneous positions of atoms, and $\langle R\rangle$ is the averaged atomic positions. Once the force constant matrix is known, the dynamical matrix, D, can be obtained by:

$$D_{\kappa\alpha,\kappa'\beta}(\vec{q}) = (m_\kappa m_{\kappa'})^{-1/2}\Phi_{k\alpha,\kappa'\beta}(\vec{q}) \tag{16}$$

where m_k is the mass of k_{th} atom.

Thermal conductivity of germanene was calculated using equilibrium MD simulation based on Green-Kubo formalism [33]. Thermal conductivity was obtained as the ensemble average over twenty independent *NVE* ensembles with different initial conditions to expand the phase trajectory sampling with 1 ns correlation time length and total simulation time of 10 ns to calculate the heat current auto-correlation function (HCACF). According to the Green-Kubo formalism, thermal conductivity and HCACF are related according to Eq. (17) [33].

$$\kappa_{\alpha\beta} = \frac{1}{Vk_BT^2}\int_0^\infty \langle J_\alpha(t).J_\beta(0)\rangle dt \tag{17}$$

where V stands for the system volume defined as the equilibrium area of germanene multiplied with h. The upper limit of the integral can be approximated by τ_m that is the correlation time required for HCACF to decay to zero. J_α and J_β stand for the heat current in α and β directions, respectively. The angular brackets represent the ensemble average of HCACF. The heat current is given by

$$J(t) = \frac{d}{dt}\sum_i E_i r_i \tag{18}$$

where E_i and r_i are the total energy (kinetic and potential) and the position of atom i, respectively. Using Hardy's definition [34] the heat current can be written as:

$$J(t) = \sum_i E_i v_i + \frac{1}{2}\sum_i \left(F_{ij}.\ v_i\right) r_{ij} \tag{19}$$

where v_i is the velocity of atom i, r_{ij}=$r_j - r_i$ and F_{ij} is the force exerted by atom j on atom i.

5. Results and discussion

The optimized parameters set for the Tersoff EP model of germanene is presented in Table 2.

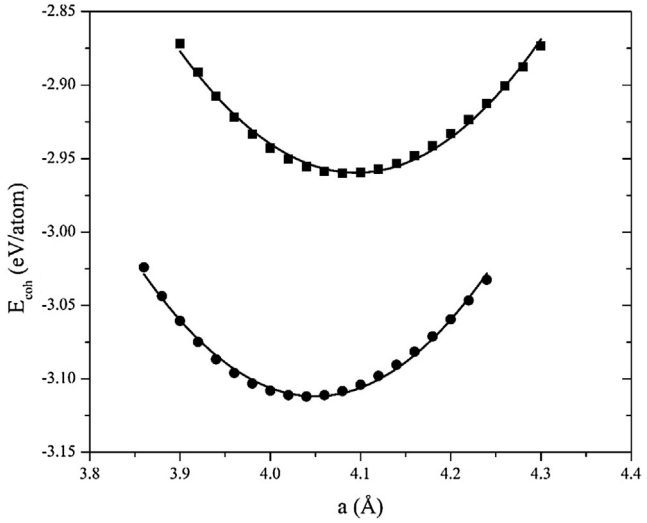

Fig. 1. Cohesive energy (E_{coh}) of germanene as a function of lattice parameter calculated using both original (square) and optimized (circle) Tersoff EPs. The buckling heights were kept constant to its original (0.48 Å) and optimized (0.73 Å) values (see Table 3).

Table 3
Different properties of germanene calculated using the original and optimized Tersoff EPs. The corresponding DFT data are also presented.

Properties	Original	Optimized	DFT
Bond length (Å)	2.43	2.43	2.44 [13]
Bond angle (°)	115.0	112.9	113 [6]
Buckling height (Å)	0.48	0.73	0.74 [14]
Lattice constant (Å)	4.10	4.05	4.06 [13]
Cohesive energy (eV/atom)	−2.95	−3.11	−3.09 [35]
E_{2g} G band (cm^{-1})	162	295	286 [36]
A_{1g} D band (cm^{-1})	164	267	265 [36]
Gruneisen parameter (G band)	−8.07	1.56	1.52 [37]
C_{11} (N m^{-1})	72.75	61.07	59.5 [38]
C_{12} (N m^{-1})	10.14	11.16	19.5 [38]
In-plane stiffness (N m^{-1})	71.3	59.0	53 [38]
Young modulus (GPa)	169.0	139.9	125.6 [38]
Poisson's ration	0.14	0.18	0.33 [31]
Heat capacity (kJ K^{-1} m^{-3})	1632	1524	1380 [21]
Thermal conductivity (W m^{-1} K^{-1})	1.7	8.9	10.5 [21]

Fig. 1 presents the cohesive energy of germanene as a function of lattice parameter calculated using both original and optimized Tersoff EPs. As this figure shows the cohesive energy (−3.11 eV/atom) and equilibrium lattice parameter (4.05 Å) were calculated using optimized Tersoff EP (the original values were calculated to be −2.95 eV/atom and 4.10 Å, respectively) are in better agreement with DFT results of −3.09 eV/atom [35] and 4.06 Å [13], respectively. Other structural properties like bond length, bond angle, and buckling height calculated using optimized Tersoff EP are also in better agreement with DFT data rather than the original ones (Table 3). Fig. 2 shows a snapshot of simulation box with both original and optimized potential parameters.

Fig. 3 presents the 3D plot of strain energy as a function of strain applied in X and Y directions. The elastic tensors, in-plane stiffness, Young modulus, and Poisson's ratio of germanene were calculated using the fitting procedure described before with both original and optimized Tersoff EPs. The results were presented in Table 3 which the DFT data are also included for comparison. As Table 3 shows, the optimized potential yields a significant improvement in estimated mechanical and elastic properties of germanene.

The phonon dispersions of germanene calculated using both original and optimized Tersoff EPs are illustrated in Fig. 4 and DFT results are also presented for comparison [36]. As Fig. 4 shows, the

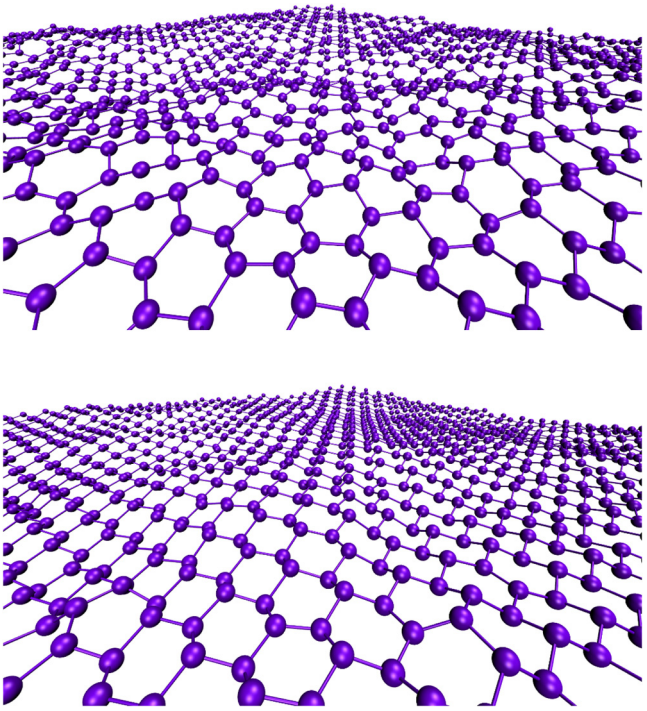

Fig. 2. Snapshot of simulation box with both original (top) and optimized (bottom) potential parameters.

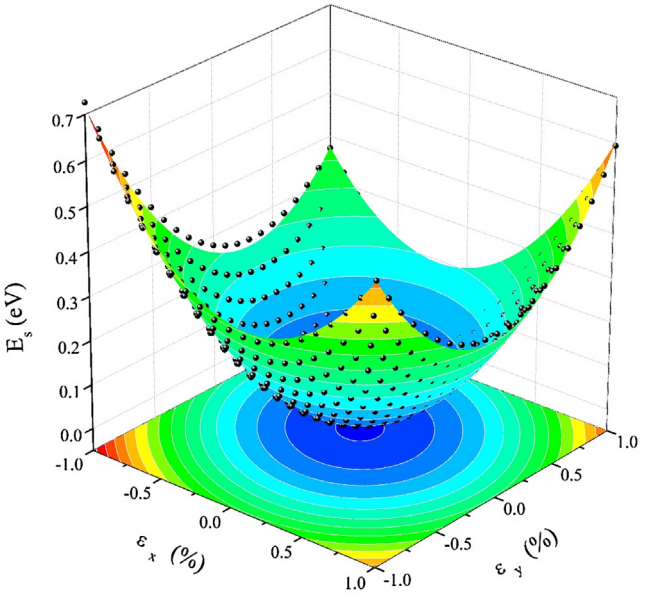

Fig. 3. 3D plot of strain energy (E_s) as a function of strain applied in X (ε_x) and Y (ε_y) directions. Black circles are the actual calculated points.

optimized Tersoff EP makes a notable improvement in phonon dispersion relation especially at high frequency optical branches. For example, the phonon frequency of E_{2g} mode (G band) at Γ point and A_{1g} mode (D band) at K point is 295 and 267 cm^{-1}, respectively that are in a good agreement with those of DFT calculations [36], namely, 286 cm^{-1} (E_{2g}) and 265 cm^{-1} (A_{1g}). However, the fitting performance in low frequency acoustic branches is not as good as optic branches especially near the K point. The inability to simultaneously fit the acoustic and optic branches is a consequence of the Tersoff EP's short range with only second-nearest-neighbor interactions represented [27].

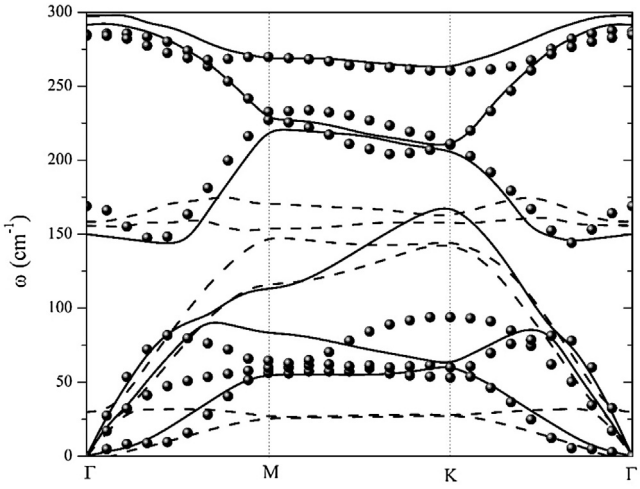

Fig. 4. Phonon dispersions of germanene calculated using both original (dashed line) and optimized (solid line) Tersoff EPs. DFT data was presented with circles [36].

The rate of change in frequency as a function of strain for a given phonon mode is determined by its Grüneisen parameter γ_g. It is a crucial parameter to quantify the rate of the phonon mode softening (stiffening) under tensile (compressive) strain and determines the thermo-mechanical properties [37]. The Grüneisen parameter is difficult to study under uniaxial stain due to the fact that it requires the Poisson ratio, which in fact depends on the choice of the substrate [17]. In presence of biaxial strain, the Grüneisen parameter γ_g for a particular band m read as [37]:

$$\gamma_g = -\frac{1}{2\omega_m^0}\frac{\partial\omega_m}{\partial\varepsilon} \tag{20}$$

where ω_m^0 and ω_m correspond to the phonon frequencies at zero strain and in the presence of biaxial strain, respectively. The Grüneisen parameter of G mode was considered here to compare with DFT results [37]. The maximum biaxial strain applied is 7% with strain rate of 0.01 ps^{-1}. The Grüneisen parameter of G mode was calculated to be 1.56 and −8.07 using optimized and original Tersoff EPs, respectively. The DFT data for Grüneisen parameter of germanene is reported to be 1.52 [37].

Heat capacity is another thermodynamic properties that was considered here. Heat capacity was calculated according to the total energy variations with temperature up to 500 K. Heat capacity calculated using the original and optimized Tersoff EPs are 1632 and 1524 kJ K^{-1} m^{-3}, respectively. Heat capacity estimated using DFT calculations was reported to be 1380 kJ K^{-1} m^{-3} [21].

As phonon dispersion calculated using the optimized Tersoff EP is in a better agreement with DFT one, it is expected that the lattice thermal conductivity estimated from optimized potential also be in a better agreement with DFT data compared with the original potential. Hence, thermal conductivity of $30 \times 30 \times 1$ super-cell germanene was calculated using equilibrium MD simulation based on Green-Kubo formalism as described before. The original and optimized Tersoff EPs result thermal conductivity of 1.7 and 8.9 W m^{-1} K^{-1}, respectively. Kuang et al. [21] was calculated the thermal conductivity of germanene using DFT method to be about 10 W m^{-1} K^{-1}.

6. Conclusion

The optimized parameter set of Tersoff empirical potential model for germanene is presented here. The well-known chi-square minimization procedure was used to optimize the original

Tersoff potential parameters. The optimized Tersoff potential has been demonstrated to notably improve the agreement between the many structural, thermodynamic, mechanical, and thermal properties of geramanene and the corresponding DFT data. According to the results, the optimized Tersoff potential presented in this work could be successfully applied for MD based studies on germanene and germanene nanoribbons.

References

[1] B. Peng, H. Zhang, H. Shao, Y. Xu, H. Zhu, $ Ab $ $ initio $ study of phonon-transport properties of two-dimensional group-IV materials. arXiv preprint arXiv:1602.02266 (2016).
[2] A.C. Ferrari, F. Bonaccorso, V. Fal'Ko, K.S. Novoselov, S. Roche, P. Bøggild, et al., Science and technology roadmap for graphene, related two-dimensional crystals, and hybrid systems, Nanoscale 7 (2015) 4598–4810.
[3] K.S. Novoselov, V.I. Fal, L. Colombo, P.R. Gellert, M.G. Schwab, K. Kim, A roadmap for graphene, Nature 490 (2012) 192–200.
[4] D. Akinwande, N. Petrone, J. Hone, Two-dimensional flexible nanoelectronics, Nat. Commun. 5 (2014).
[5] J. Hu, Z. Guo, P.E. McWilliams, J.E. Darges, D.L. Druffel, A.M. Moran, et al., Band gap engineering in a 2D material for solar-to-chemical energy conversion, Nano Lett. 16 (2015) 74–79.
[6] C. Lee, X. Wei, J.W. Kysar, J. Hone, Measurement of the elastic properties and intrinsic strength of monolayer graphene, Science 321 (2008) 385–388.
[7] S.D. Sarma, S. Adam, E.H. Hwang, E. Rossi, Electronic transport in two-dimensional graphene, Rev. Mod. Phys. 83 (2011) 407.
[8] S.J. Mahdizadeh, E.K. Goharshadi, Thermal conductivity and heat transport properties of graphene nanoribbons, J. Nanopart. Res. 16 (2014) 1–12.
[9] M.E. Dávila, L. Xian, S. Cahangirov, A. Rubio, G. Le Lay, Germanene: a novel two-dimensional germanium allotrope akin to graphene and silicene, N. J. Phys. 16 (2014) 095002.
[10] H.-S. Tsai, Y.-Z. Chen, H. Medina, T.-Y. Su, T.-S. Chou, Y.-H. Chen, et al., Direct formation of large-scale multi-layered germanene on Si substrate, Phys. Chem. Chem. Phys. 17 (2015) 21389–21393.
[11] M.E. Dávila, G. Le Lay, Few layer epitaxial germanene: a novel two-dimensional Dirac material, Sci. Rep. 6 (2016).
[12] A. Dimoulas, Silicene and germanene: silicon and germanium in the flatland, Microelectron. Eng. 131 (2015) 68–78.
[13] F. Matusalem, M. Marques, L.K. Teles, F. Bechstedt, Stability and electronic structure of two-dimensional allotropes of group-IV materials, Phys. Rev. B 92 (2015) 045436.
[14] A. Acun, L. Zhang, P. Bampoulis, M. Farmanbar, A. Van Houselt, A.N. Rudenko, et al., Germanene: the germanium analogue of graphene, J. Phys.: Condens. Matter 27 (2015) 443002.
[15] Z. Ni, Q. Liu, K. Tang, J. Zheng, J. Zhou, R. Qin, et al., Tunable bandgap in silicene and germanene, Nano Lett. 12 (2011) 113–118.
[16] B. Bishnoi, B. Ghosh, Spin transport in silicene and germanene, RSC Adv. 3 (2013) 26153–26159.
[17] T.P. Kaloni, U. Schwingenschlögl, Stability of germanene under tensile strain, Chem. Phys. Lett. 583 (2013) 137–140.
[18] N.J. Roome, J.D. Carey, Beyond graphene: stable elemental monolayers of silicene and germanene, ACS Appl. Mater. Interfaces 6 (2014) 7743–7750.
[19] T.P. Kaloni, Tuning the structural, electronic, and magnetic properties of germanene by the adsorption of 3d transition metal atoms, J. Phys. Chem. C 118 (2014) 25200–25208.
[20] L.-F. Huang, P.-L. Gong, Z. Zeng, Phonon properties, thermal expansion, and thermomechanics of silicene and germanene, Phys. Rev. B 91 (2015) 205433.
[21] Y.D. Kuang, L. Lindsay, S.Q. Shi, G.P. Zheng, Tensile strains give rise to strong size effects for thermal conductivities of silicene, germanene and stanene, Nanoscale 8 (2016) 3760–3767.
[22] U. Monteverde, M.A. Migliorato, J. Pal, D. Powell, Elastic and vibrational properties of group IV semiconductors in empirical potential modelling, J. Phys.: Condens. Matter 25 (2013) 425801.
[23] J. Tersoff, Modeling solid-state chemistry: interatomic potentials for multicomponent systems, Phys. Rev. B 39 (1989) 5566.
[24] J. Tersoff, New empirical approach for the structure and energy of covalent systems, Phys. Rev. B 37 (1988) 6991.
[25] J. Tersoff, Empirical interatomic potential for carbon, with applications to amorphous carbon, Phys. Rev. Lett. 61 (1988) 2879.
[26] A. Kınacı, J.B. Haskins, C. Sevik, T. Çağın, Thermal conductivity of BN-C nanostructures, Phys. Rev. B 86 (2012) 115410.
[27] L. Lindsay, D.A. Broido, Optimized Tersoff and Brenner empirical potential parameters for lattice dynamics and phonon thermal transport in carbon nanotubes and graphene, Phys. Rev. B 81 (2010) 205441.
[28] D. Powell, M.A. Migliorato, A.G. Cullis, Optimized Tersoff potential parameters for tetrahedrally bonded III–V semiconductors, Phys. Rev. B 75 (2007) 115202.
[29] W.H. Press, Numerical Recipes 3rd Edition: The Art of Scientific Computing, Cambridge University Press, 2007.
[30] S. Plimpton, Fast parallel algorithms for short-range molecular dynamics, J. Comput. Phys. 117 (1995) 1–19.
[31] H. Şahin, S. Cahangirov, M. Topsakal, E. Bekaroglu, E. Akturk, R.T. Senger, et al., Monolayer honeycomb structures of group-IV elements and III–V binary compounds: first-principles calculations, Phys. Rev. B 80 (2009) 155453.
[32] L.T. Kong, G. Bartels, C. Campañá, C. Denniston, M.H. Müser, Implementation of green's function molecular dynamics: an extension to LAMMPS, Comput. Phys. Commun. 180 (2009) 1004–1010.
[33] S.J. Mahdizadeh, E.K. Goharshadi, G. Akhlamadi, Thermo-mechanical properties of boron nitride nanoribbons: a molecular dynamics simulation study, J. Mol. Graph. Modell. 68 (2016) 1–13.
[34] R.J. Hardy, Energy-flux operator for a lattice, Phys. Rev. 132 (1963) 168.
[35] T.P. Kaloni, G. Schreckenbach, M.S. Freund, U. Schwingenschlögl, Current developments in silicene and germanene, Phys. Status Solidi (RRL)-Rapid Res. Lett. 10 (2016) 133–142.
[36] S.J. Zaveh, M.R. Roknabadi, T. Morshedloo, M. Modarresi, Electronic and thermal properties of germanene and stanene by first-principles calculations, Superlattices Microstruct. 91 (2016) 383–390.
[37] J.-A. Yan, S.-P. Gao, R. Stein, G. Coard, Tuning the electronic structure of silicene and germanene by biaxial strain and electric field, Phys. Rev. B 91 (2015) 245403.
[38] S. Balendhran, S. Walia, H. Nili, S. Sriram, M. Bhaskaran, Elemental analogues of graphene: silicene, germanene, stanene, and phosphorene, Small 11 (2015) 640–652.